Biomimetic evaluation of β tricalcium phosphate prepared by hot isostatic pressing

Mihaela Mateescu, Emmanuelle Rguitti, Arnaud Ponche, Michel Descamps, Karine Anselme

Biomatter

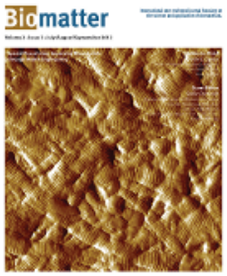

ISSN: (Print) 2159-2535 (Online) Journal homepage: http://www.tandfonline.com/loi/kbim20

Biomimetic evaluation of β tricalcium phosphate prepared by hot isostatic pressing

Mihaela Mateescu, Emmanuelle Rguitti, Arnaud Ponche, Michel Descamps & Karine Anselme

To cite this article: Mihaela Mateescu, Emmanuelle Rguitti, Arnaud Ponche, Michel Descamps & Karine Anselme (2012) Biomimetic evaluation of β tricalcium phosphate prepared by hot isostatic pressing, Biomatter, 2:3, 103-113, DOI: 10.4161/biom.21377

To link to this article: https://doi.org/10.4161/biom.21377

Published online: 01 Jul 2012.

Biomatter 2:3, 103–113; July/August/September 2012; © 2012 Landes Bioscience

Biomimetic evaluation of β tricalcium phosphate prepared by hot isostatic pressing

Mihaela Mateescu,[1,*] Emmanuelle Rguitti,[2] Arnaud Ponche,[1] Michel Descamps[2] and Karine Anselme[1]

[1]Institut de Science des Matériaux de Mulhouse (IS2M); CNRS LRC7228; Mulhouse, France; [2]Laboratoire des Matériaux Céramiques et Procédés Associés (LMCPA); Université Lille Nord de France; Lille, France

Keywords: biomimetic, TCP, dynamic, static, osteoblast

Two types of completely densified β-TCP tablets were synthesized from a stoichiometric β-TCP powder. The first ones (TCP) were conventionally sintered, while the second ones (TCP-T) were sintered and treated by hot isostatic process (HIP). The HIP produced completely densified materials with relative densities greater than 99.9% and a transparent appearance of tablets. Samples were immersed in culture medium with (CM) or without serum (NCM) in static and dynamic conditions for a biomimetic evaluation. Similarly, SaOs-2 cells were cultured on samples in a static or dynamic flow perfusion system. The results of surface transformation in absence of cells showed that the dynamic condition increased the speed of calcium phosphate precipitations compared with the static condition. The morphology of precipitates was different with nature of tablets. The immersion in CM did impede this precipitation. XPS analysis of TCP-T tablets showed the presence of hydroxyapatite (HA) precipitates after incubation in NCM while octacalcium phosphate (OCP) precipitates were formed after incubation in CM. The analysis of the response of SaOs-2 cells on surfaces showed that the two types of materials are biocompatible. However, the dynamic mode of culture stimulated the differentiation of cells. Finally, it appears that the HIP treatment of TCP produces highly densified and transparent samples that display a good in vitro biocompatibility in static and dynamic culture conditions. Moreover, an interesting result of this work is the relationship between the presence of proteins in the immersion medium and the quality of precipitates formed on hipped TCP surface.

Introduction

β-tricalcium phosphate (β-TCP) presents an excellent biocompatibility and osteoconductiveness because its high capacity of resorption. β-TCP is generally fabricated as particles[1,2] or porous scaffolds associated in some cases with proteins,[3] polymers[4-7] or other ceramics like hydroxyapatite.[8-10] The biocompatibility of these samples has been studied in static or in dynamic conditions[3,5,11] in vitro[6,7] or in vivo.[2,12-14]

This work proposes two innovative aspects: first, we consider a new type of completely densified β-TCP samples. β-TCP ceramics present relatively poor mechanical properties, which limit their use in load bearing application. A well-known way to improve the tensile strength of ceramic is to develop materials with high densities and fine microstructures in order to reduce the size and distribution of pre-existing defects that are responsible of the material rupture. Among the most effective ceramic densification processes, hot isostatic pressing (HIP) allows full densification with a minimum grain growth. Two types of tablets were synthesized and compared in this study: TCP (pressureless sintered) and TCP-T (sintered and hipped).

Second, in order to characterize in a more pertinent manner the transformations of TCP and TCP-T surfaces in biological fluids and to evaluate their in vitro biocompatibility, we applied a previously developed biomimetic approach. The biomimetic approach consists in the immersion of samples in simulated body fluid solutions (SBF) in order to observe the surface transformations occurring on the ceramic samples. However, we recently showed that the immersion in solutions closer to the biological fluids i.e., containing proteins such as culture medium with 10% fetal calf serum (FCS) induces transformations that are not comparable to the ones obtained after immersion in SBF. Moreover, we also demonstrated that an immersion in a circulating fluid (dynamic condition) gave different surface transformation than in static condition.[15] So, in this paper, we performed (1) the replacement of SBF by a cell culture medium containing (complete medium) or not (non-complete medium) 10% of proteins from FCS, (2) the application of dynamic forces with a fluid perfusion system (2 ml/h, the physiological rate in bone tissue) and (3) in conditions mimicking the main features of blood serum: pH = 7.4 and 37°C under p(CO2) = 0.05 atm (5%). That parameters lead to a better simulation of the conditions the samples are submitted in vivo making the assay more predictive and reliable.

Moreover, we also recently showed that in vitro biocompatibility tests gave different results when the cultures were done in

*Correspondence to: Mihaela Mateescu; Email: miamateescu@gmail.com
Submitted: 02/14/12; Revised: 06/26/12; Accepted: 07/05/12
http://dx.doi.org/10.4161/biom.21377

dynamic condition.[16] The adhesion of human osteoblastic cells on Si-HA doped dense ceramic tablets as well as their alkaline phosphatase activity was faster and stronger in dynamic culture conditions than in static culture conditions the demonstrating again the interest to use also a biomimetic approach to evaluate the biocompatibility of biomaterials.

Finally, the aims of the present study are to compare for the two types of tablets: TCP and TCP-T (1) the surface transformation of samples and (2) SaOs-2 osteoblastic activity, in conventional static condition and in a dynamic flow perfusion system.

Results

Characterization of TCP powders. X-ray diffraction spectrum of final TCP powders showed no foreign phases (**Fig. 1A**). No trace of HA appeared on the TCP spectra. Except the peaks at 3,460 and 1,650 cm^{-1} (that can be attributed to adsorbed H_2O and CO_2), all the bands in the FTIR spectrum (**Fig. 1B**) corresponded to PO_4^{3-} groups. The characteristic bands of calcium pyrophosphate ($Ca_2P_2O_7$) (at 723, 1,185 and 1,210 cm^{-1}), which appears when the Ca/P ratio < 1.5, were not observed. This analysis, which can detect quantities of $Ca_2P_2O_7$ lower than 0.1 wt.% in the TCP, demonstrates that the TCP powder was free of calcium pyrophosphate.

The specific surface area of the TCP powder after calcination and ball milling treatment was equal to 7 m^2/g.

Pressureless sintering and HIP treatments of TCP tablets. After a pressureless sintering at 1,060°C, TCP tablets presented a relative density of 98.5% with completely closed residual porosity, (necessary condition for further densification by HIP). The as

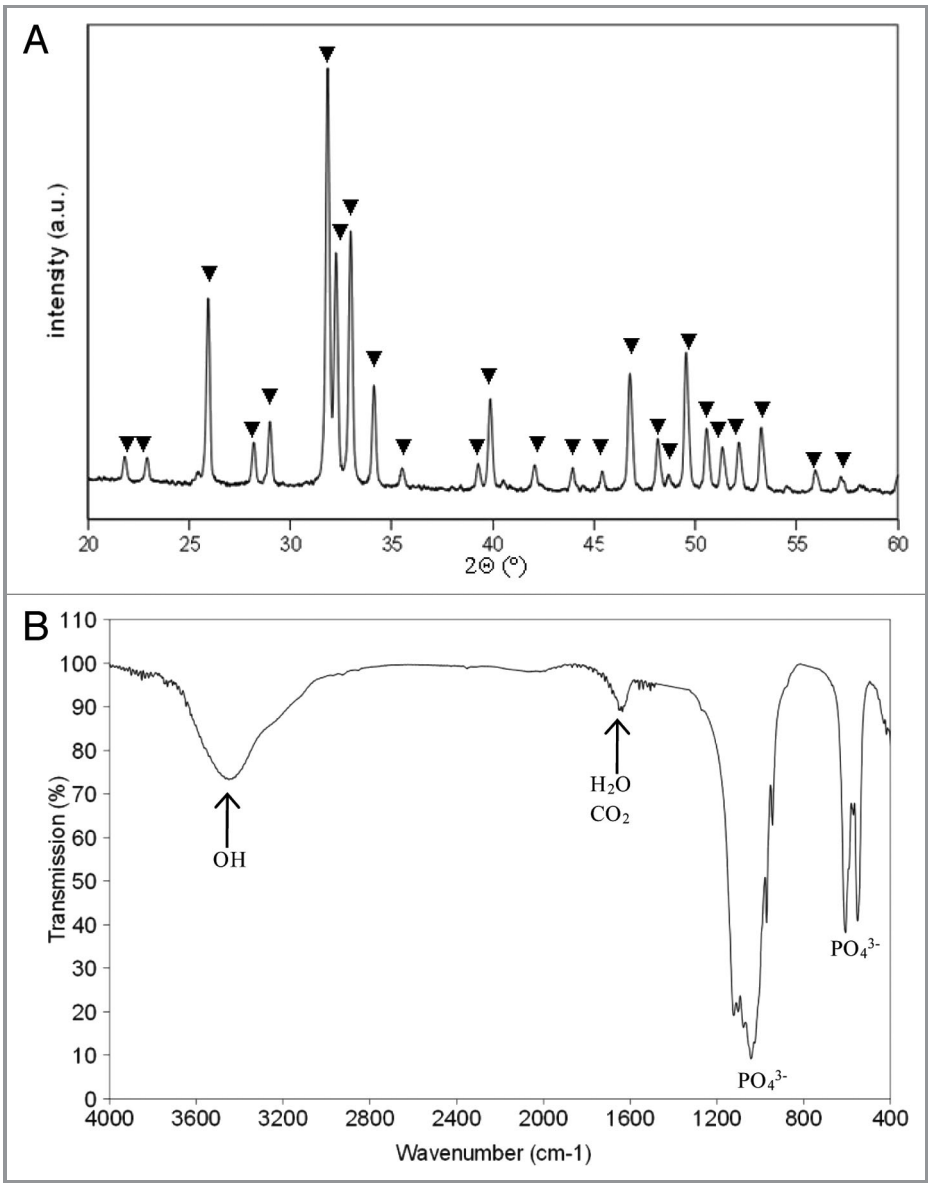

Figure 1. (A) XRD patterns of β-TCP powder (▼); (B) IR spectra of β-TCP powder.

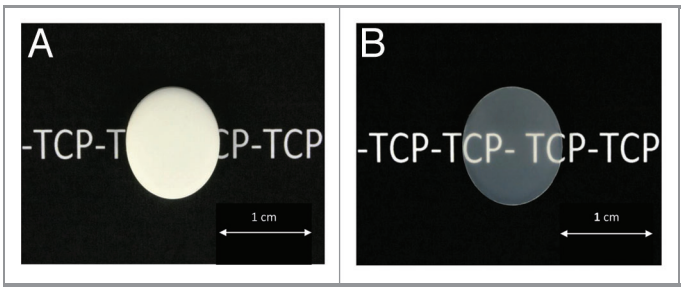

Figure 2. Photographs illustrating the transparency of TCP-T samples (B) compared with TCP (A).

pre-sintered TCP compacts were hipped to 1,050°C during 1 h. Samples obtained after this treatment were completely densified with relative densities greater than 99.9%. Moreover, these samples exhibited after polishing a transparent appearance (**Fig. 2**).

This transparent appearance indicates that the densities of these materials were close to the theoretical density. Indeed a major detrimental factor to transparency of ceramic materials is the residual porosity. On the contrary, the grain size of TCP measured for pressureless sintered and hipped samples were similar and ranged from 0.5 to 1.5 µm (**Fig. 3**). Similarly, X-ray diffraction and IR spectra of hipped specimens did not show any change compared with pre-sintered materials.

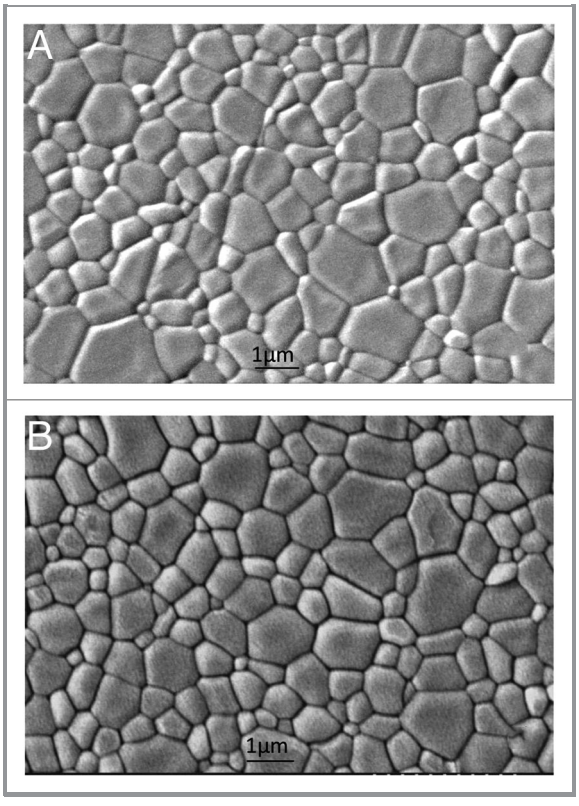

Figure 3. Initial SEM micrographs of TCP (A) and TCP-T (B) samples.

Surface modifications during biomimetic immersion. **Figure 4** presents the surface transformation of the materials after immersion during 3 and 8 d in static and dynamic conditions, in the presence of NCM and CM. After immersion in biological fluid, a formation of precipitated particles was observed notably in absence of proteins. The quantity of precipitates increased with time of immersion like classically observed[17] and was higher in dynamic than in static conditions [see for example, TCP-T 3 d in non-complete medium (NCM)]. TCP-T showed accelerated faster precipitation compared with TCP. TCP immersed in static condition was not completely covered with particles after 8 d contrary to TCP-T. A difference in morphology of precipitated particles was visible on TCP between static and dynamic immersion conditions. On TCP, the particles were denser and more spherical in static than in dynamic conditions. On TCP-T, the immersion during 8 d in static conditions provoked the precipitation of homogenous layers of apatite crystals although in dynamic conditions, the formation of particles was rather observed. However, the apatite layers were denser and deposited faster on TCP-T than on TCP whatever the immersion conditions.

The immersion in medium containing proteins did impede the precipitation of apatite. On the surfaces immersed in complete medium, particles measuring several micrometers in diameter were frequently observed. The presence of a precipitated apatite particleslayer was visible only on TCP-T after 8 d of dynamic immersion in CM. Some particles were also observed but their morphology was however different than the ones observed on TCP-T immersed in NCM.

The variation of calcium, phosphate and proteins contents of immersion media during the time were not modified (data not shown) whatever applied the conditions. This is probably due to the low sensitivity of these chemical methods.

The EDX and XPS analysis were performed to explore surface chemical modifications after biomimetic study. The EDX spectra give information on the surface chemical composition over a probing depth of approximately 1 µm. We were particularly interested in the difference in chemical compositions between the precipitated layer covering the samples and the particles formed on the surface of this layer (**Table 1**). The Ca/P ratio of the particles was systematically lower than the one of the layer whatever the immersion condition and medium.

The atomic concentrations of elements and the Ca/P, O/Ca and $O_{(1s)II}/O_{(1s)total}$ atomic ratios obtained from XPS measurements were calculated (**Table 2**). In comparison, the experimental Ca/P, O/Ca and $O_{(1s)II}/O_{(1s)total}$ ratios measured by Lu et al.[18] on synthesized and finely characterized HA, β-TCP, OCP, MCP, DCP, DCPD and pig cortical bone tablets are grouped in the **Table 3**. These values will be useful for distinguishing the six important biologically calcium phosphate phases: HA, β-TCP, DCPD, DCP, MCP, OCP that could coexist on the TCP-T samples after 8 d of immersion in CM and NCM fluids under static and dynamic conditions. The values calculated by Lu et al.[18] seem really appropriate to calculate our phases since the Ca/P ratio of TCP-T control (Ca/P = 1.23) was closer to Lu et al.'s value (Ca/P = 1.35) than the theoretical value (Ca/P = 1.5). As Lu

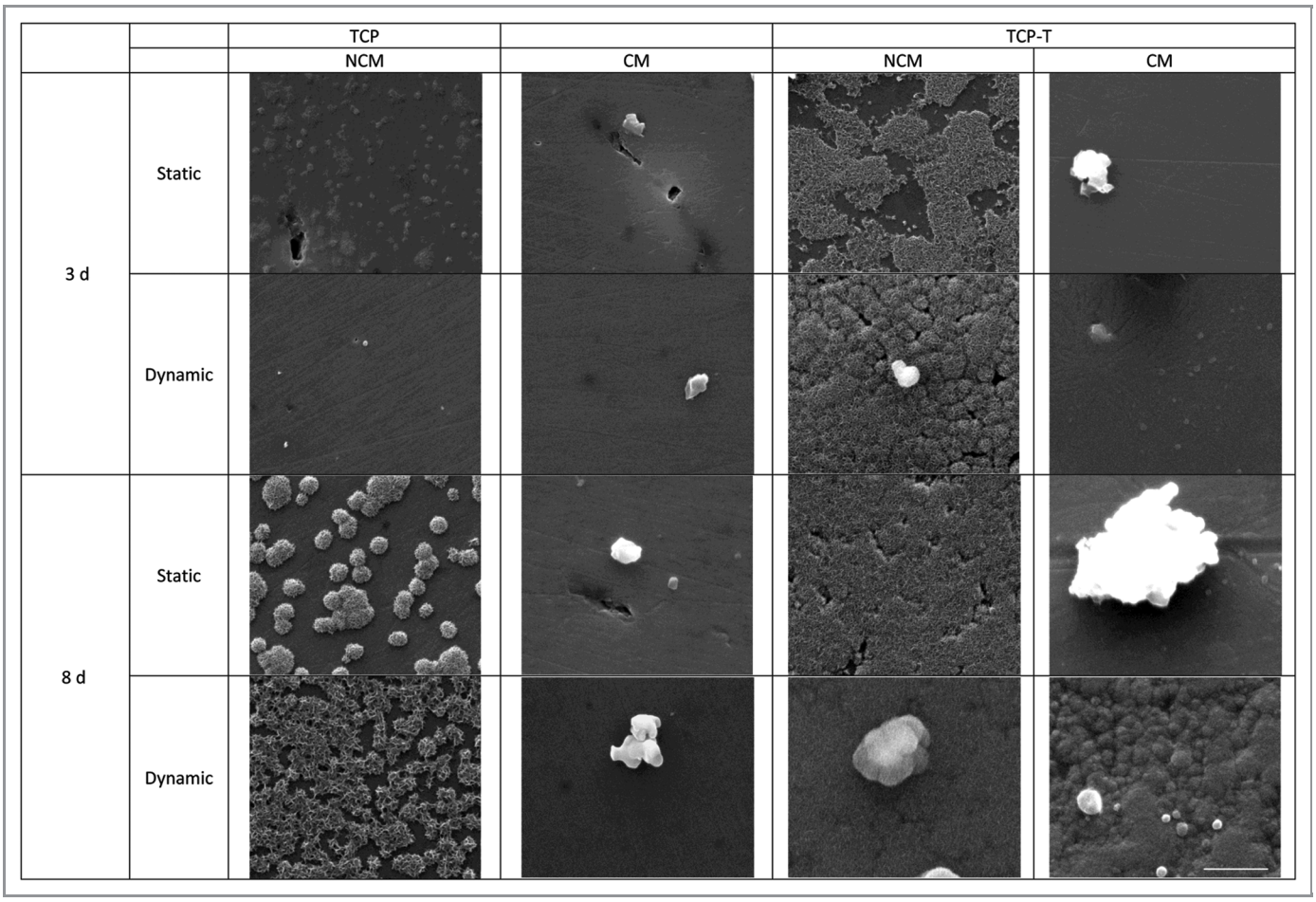

Figure 4. SEM micrographs of TCP and TCP-T samples after biomimetic study (bar = 5 μm).

Table 1. EDX Ca/P ratio of TCP and TCP-T samples before and after 3 and 8 d of biomimetic study

	TCP	NCM		CM	
		Static	Dynamic	Static	Dynamic
		Ca/P			
3 d	Control	1.40	1.40	1.40	1.40
	Particles	1.36	1.42	1.28	1.36
	Precipitated layer	1.43	1.44	1.41	1.43
8 d	Particles	1.37	1.26	1.29	1.25
	Precipitated layer	1.41	1.49	1.41	1.44
	TCP-T	**NCM**		**CM**	
		Static	**Dynamic**	**Static**	**Dynamic**
		Ca/P			
3 d	Control	1.41	1.41	1.41	1.41
	Particles	1.40	1.37	1.29	1.41
	Precipitated layer	1.45	1.46	1.39	1.49
8 d	Particles	1.40	1.29	1.29	1.30
	Precipitated layer	1.44	1.44	1.46	1.49

et al.'s value of Ca/P is slightly different form our experimental Ca/P ratio, all our ratio values were modified by a parameter "r" representing the deviation between our control values and Lu et al.[18] Moreover, they developed an original method based on the study of the O1s loss spectrum to identify phases that we applied to our samples (see **Fig. 5**).

The parameter "r" for each ratio is calculated as follow: the $r_{Ca/P}$ = 1.35/1.23 = 1.097; $r_{O/C}$ = 2.72/2.38 = 1.14 and $r_{O(1s)II/O(1s)total}$ = 0.072/0.056 = 1.28. **Table 4** presents the modified values [calculated by multiplying the parameter "r" with the initial values of Ca/P, O/C and $O_{(1s)II}/O_{(1s)total}$ ratio]. Ca/P, O/C and $O_{(1s)II}/O_{(1s)total}$ ratio, calculated for the NCM and CM conditions in static and dynamic experiments, are sensitive to the phases detected at the surface of TCP-T. On the basis of Lu et al.[18] values, it is then possible to give a chemical interpretation of the phases present at the extreme surface (9 nm with XPS measurment) of TCP substrates where dissolution and precipitation reaction occurs.

Biomimetic cell study. The adhesion of SaOs-2 cells on TCP and TCP–T after 3 d in static and dynamic conditions showed a normal spreading with mature actin cytoskeleton fibers (**Fig. 6**). No significant difference was observed between the samples.

Table 2. Chemical composition (at.%) and atomic ratios for TCP-T samples in dynamic and static conditions, determinated from XPS analysis

	TCP-T	P 2p	C 1s	Ca 2p	N 1s	O 1s	Na 1s	Mg 2p	Ca/P	O/Ca	O(1s)II/O(1s)total
	Control	16.09	14.98	19.79	0	47.19	0	0	1.23	2.38	0.056
NCM	Static	14.64	20.78	18.91	0.84	45.82	0.2	1.3	1.29	2.42	0.054
	Dynamic	14.01	21.27	18.69	0.69	45.3	0.23	0.8	1.33	2.42	0.052
MC	Static	7.74	44.83	8.71	7.16	31.56	0	0	1.13	3.62	0.024
	Dynamic	7.64	45.09	8.4	7.64	31.24	0	0	1.10	3.72	0.037

The number of viable cells was comparable on TCP and TCP-T in static and dynamic culture conditions after 1 and 3 d. After 7 d, the number of cells was higher on TCP than on TCP-T samples whatever the culture conditions (**Fig. 7A**). Concerning the differentiation of cells, their alkaline phosphatase activity was equal after 1 and 3 d of incubation and higher on TCP-T than on TCP after 7 d whatever the culture conditions (**Fig. 7B**).

Discussion

Surface modifications during biomimetic immersion. In general, the particles observed on TCP plates are composed by nucleated apatite crystallites like previously observed by Juhasz et al.[19] after immersion of TCP in SBF. It is classically considered that a higher dissolution is the reason of an increased precipitation but this is only true for materials able to dissolve in SBF. This is not true for TCP that is insoluble in SBF.[20]

The increase in material surface area in contact with chemical or biological fluids, which promotes ceramic dissolution, could also be an explanation for more precipitation. For example, powders with high specific surface or significant microporosity would have higher contact area with fluids. However, in our case, the two materials are in a compact form with identical surfaces and can be considered as not microporous and notably TCP-T that was completely densified after HIP. Microstructure and especially the grain size of material could also impact the precipitation phenomenon. Indeed, it was shown that the preferential grain boundaries dissolution can play a significant role in increasing the dissolution rate of material.[21] However, in our case, the size of grains was similar for the two materials.

Moreover, the calcium and phosphate contents of immersion media were not modified demonstrating the low dissolution rate of the two materials (data not shown). More probably, as proposed by Bohner and Lemaitre, TCP could induce apatite precipitation because it provides a surface with a low interfacial energy with apatite.[20] Thus, the higher apatite precipitation on TCP-T would be related to a lower interfacial energy of TCP-T compared with TCP. The fact that the apatite crystals were larger and deposited faster on TCP-T than on TCP is surely related to the HIP procedure that changes the nanostructure of TCP-T samples improving the ceramic densification by decreasing the porosity. The dynamic conditions increased the precipitation speed compared with static conditions. This is in contradiction with results obtained by Vallet-Regi et al.,[22] but they performed experiments on glass, in presence of SBF and with a flow rate of 1 ml/min. At 1 ml/min the precipitation process may be impeded by the flow rate that was largely higher than in our experiment (2 ml/h). Moreover, the mechanisms of nucleation consist in the interchange of ions like Ca^{+2} or PO_4^{3-} of ceramics samples with soaking medium. In dynamic conditions, the nuclei may grow more rapidly because the quantity of ions in the solution is continuously changed whereas in static conditions, the solution remains the same during the experiment.

Table 3. Direct Ca/P, O/Ca and O(1s)II/O(1s) total ratio given by Lu et al.[18]

Sample	HAP	β-TCP	OCP	MCP	DCP	DCPD	Bone
Ca/P	1.48	1.35	1.24	0.5	1	0.98	1.49
O/Ca	2.76	2.72	3.4	10.38	4.3	5.4	3.2
$O_{(1s)II}/O_{(1s)total}$	0.065	0.072	0.053	0.008	0.037	0.02	0.055

HAP, hydroxyapatite: $Ca_{10}(OH)_2(PO_4)_6$; β-TCP, β-tricalcium phosphate: $Ca_3(PO_4)_2$; OCP, octacalcium phosphate: $Ca_8H_2(PO_4)_6$; MCP, monobasic calcium phosphate: $Ca(H_2PO_4)_2$; DCP, dibasic calcium phosphate: $CaHPO_4$; DCPD, dibasic calcium phosphate dihydrate, brushite: $CaHPO_4 \cdot 2H_2O$.

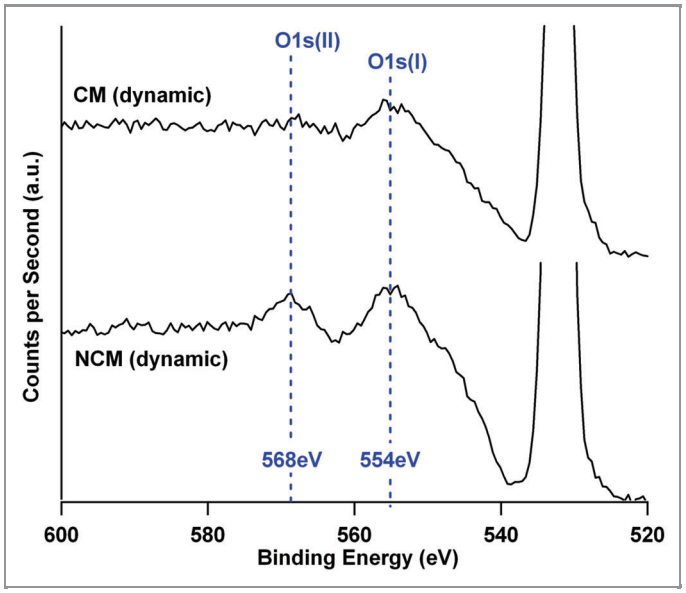

Figure 5. O1s loss spectrum of TCP-T ceramic after 8 d in NCM and CM culture media in dynamic conditions. The O1s photoelectric peak is located at 532 eV. The area ratio between the two components of the loss spectrum (554 eV and 568 eV) are modified by the culture conditions indicating a modification of the ceramic phases. The two spectra are represented with the same ordinate scale.

Table 4. Identification of CaP phases for TCP-T samples after normalization from values given by Lu et al.[18]

	TCP-T	Ca/P	Newly calculated Ca/P	Phase identification	O/Ca	Newly calculated O/Ca	Phase identification	O(1s)II/O(1s)total	Newly calculated O(1s)II/O(1s)total	Phase identification
	Control	1.23	1.35	β-*TCP*	2.38	2.73	β-*TCP*	0.056	0.072	β-*TCP*
NCM	Static	1.29	1.42	*HA*	2.42	2.77	*HA*	0.054	0.069	*HA*
	Dynamic	1.33	1.46	*HA*	2.42	2.77	*HA*	0.052	0.067	*HA*
CM	Static	1.13	1.24	*OCP*	3.62	4.14	*DCP*	0.024	0.031	*DCP*
	Dynamic	1.10	1.21	*OCP*	3.72	4.25	*DCP*	0.037	0.048	*OCP*

O1s(I) and O1s(II) components are due to the loss spectrum of O1s and are located respectively to 554 eV and 568 eV.

As previously described the immersion in medium containing proteins did impede the precipitation of apatite crystals.[19,20,23,24] With microBCA test (data not shown) we did not observe a significant protein adsorption on our samples surely because the low sensitivity of the method. However, the XPS analysis confirmed the presence of the N signal (complete medium: 7.2–7.6% N1s, **Table 2**) at the surface that can be related to adsorbed proteins. The apatite nucleation on TCP and TCP-T was inhibited but a precipitated layer was observed only on T-TCP after 8 d of dynamic immersion in CM. It was more close to the morphology of hydroxyapatite layers described by Juhasz et al.[19] on brushite samples immersed in human blood serum. This was interpreted as Ca^{2+} chelating properties of proteins in solution, which cause a decrease in the supersaturating state of the solution hence preventing crystal formation. It was also proposed that adsorbed proteins lead to an increase in Ca-accumulations within the surface and decreases the resulting Ca^{2+} release.[23] However, the influence of protein in the immersion medium was variable in function of the ceramic immersed. TCP showed the lowest surface transformation in protein-free and protein-containing solutions.[24] Our results confirmed these observations with TCP showing less transformation than TCP-T. This again highlights that the HIP treatment of TCP modifies its nanostructure and together its reactivity in biological fluids.

The EDX measurements show that the increase of the Ca/P ratio of the precipitated layer was higher in dynamic conditions

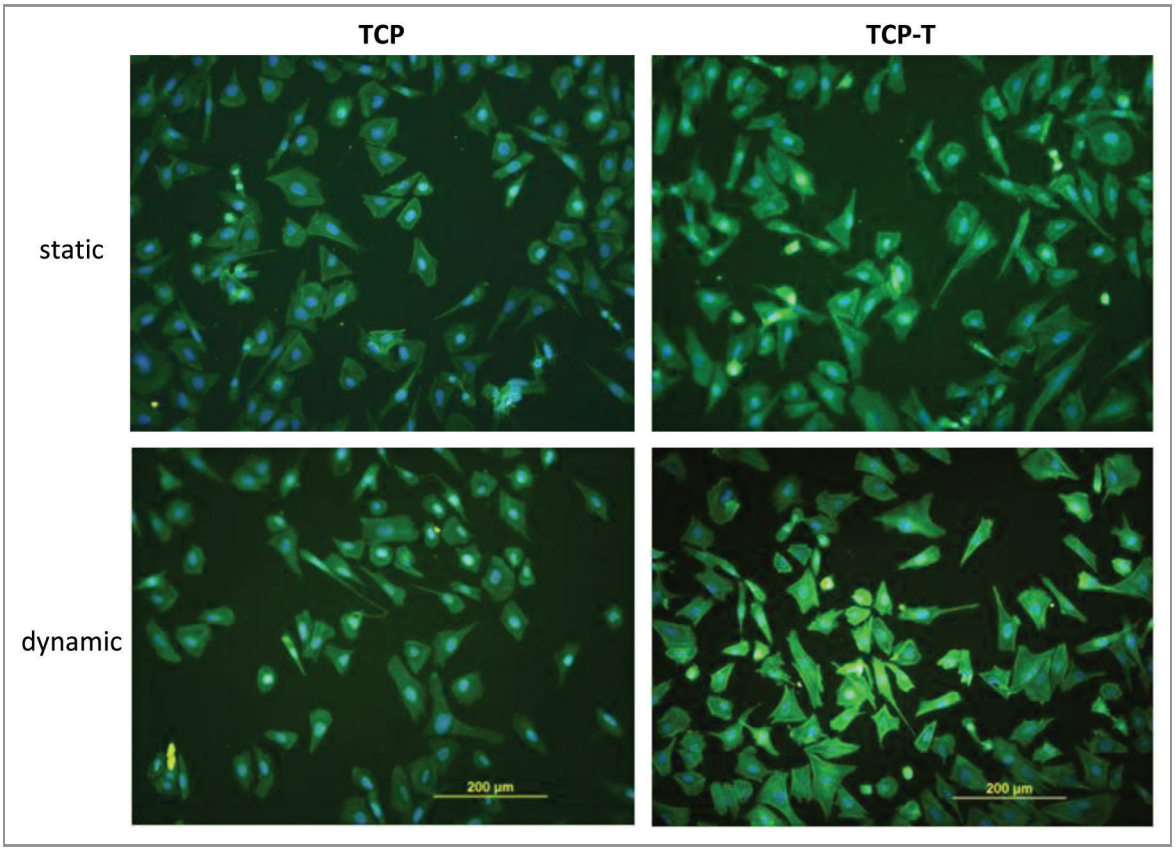

Figure 6. Fluorescence micrographs of actin cytoskeleton of SaOs-2 cells adhered after 4 d of culture on TCP and TCP-T samples in static and dynamic condition.

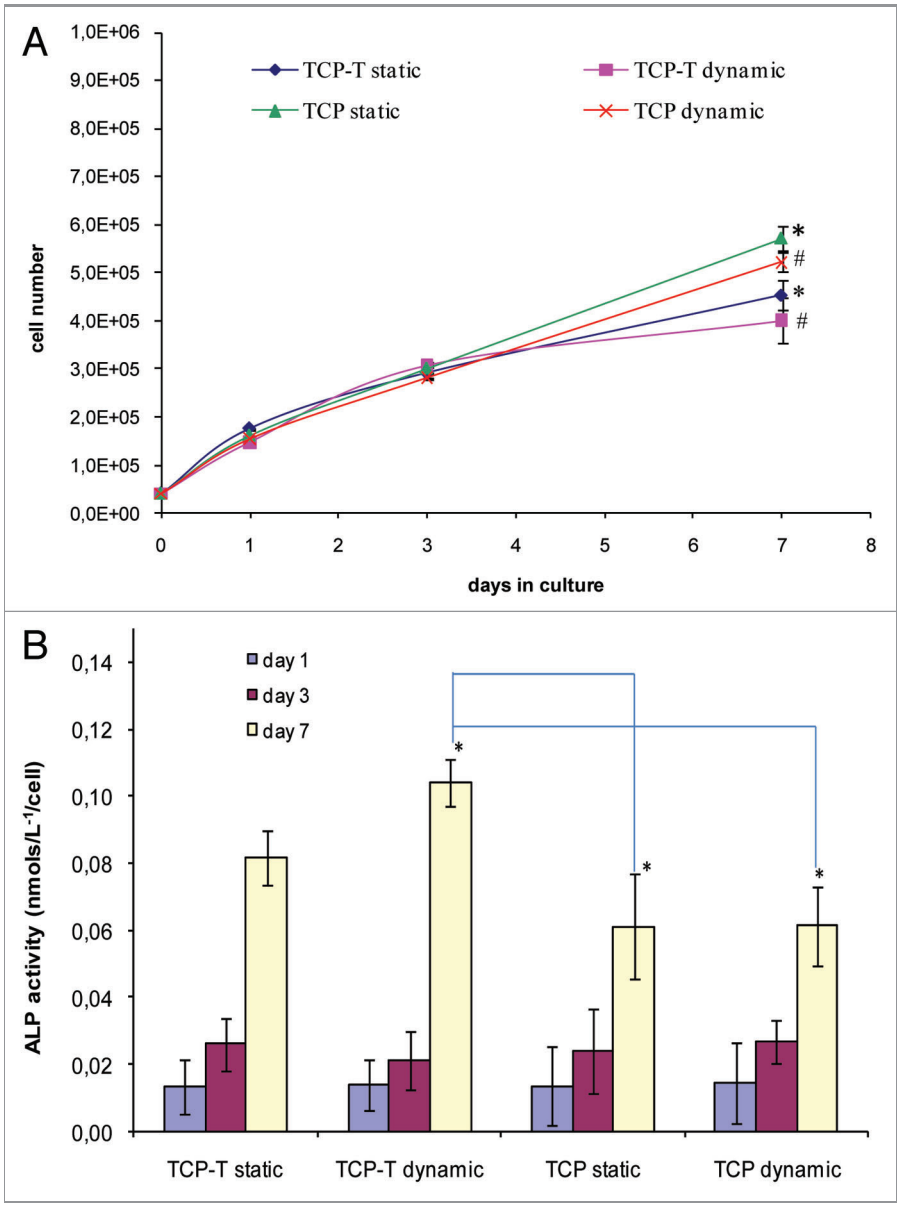

Figure 7. (A) Proliferation of SaOs-2 cells cultured on TCP and TCP-T samples in static and dynamic conditions. (B) Alkaline phosphatase activity of SaOs-2 cells cultured on TCP and TCP-T samples in static and dynamic conditions. (A) The asterisk (*) denotes a statistical difference between TCP and TCP-T in dynamic conditions and the asterisk (#) indicates a statistical difference between TCP and TCP-T in static condition after 7 d of culture ($p < 0.05$). (B) The asterisk (*) indicates a significant difference in ALP activity after 7 d between TCP-T in dynamic mode and TCP in dynamic and static mode ($p < 0.05$). Error bars represent means ± SD.

than in static conditions, compared with untreated control. That means that the newly formed apatitic layer was enriched with Ca. On the other hand, the Ca/P ratios of particles formed at the surface were lower than the ones of the apatite layer especially after 8 d in dynamic conditions. The particles did present a higher quantity of phosphate (**Table 1**). Moreover, the immersion in NCM media made particles that also contained Mg^{2+} and Na^{+} beside the Ca^{2+} and PO_4^{-3} elements (**Table 2**).

The XPS measurements of modified Ca/P and O/Ca ratios for TCP-T did indicate the presence of HA phases for NCM incubations and OCP or DCP phases for CM incubations. Therefore, in order to identify the phases in a more definitive way, the oxygen loss spectrum was analyzed. The values of $O_{(1s)II}/O_{(1s)total}$ confirmed the presence of HA phases for the NCM incubations (static or dynamic). For CM incubations, the DCP phases were present in static immersion although OCP phases were present in dynamic conditions (**Table 4**).

However, it should be noted that some of our measurements were slightly different than Lu et al.'s[18] values, this may be because of the presence of proteins in our system. The O1s loss spectrum exhibited two components for NCM immersions, located at 554eV [O1s(I)] and 568eV [O1s(II)] with a same intensity. In presence of CM, the second component, located at 568eV was attenuated (**Fig. 5**). This attenuation cannot be only explained by

the presence of the protein overlayer because O1s(II) component of the loss spectrum (554eV) was affected in a different manner than O1s(I). Then, the O1s(II)/O1s(I) ratio would be characteristic of the different phases present at the ceramic surface (phases which are modified by dissolution/precipitation reactions during immersion time). The different orientation and density of cristallographic phases induce a specific variation of the energy loss pattern obtained on O1s spectrum for CM incubations. This spectroscopic observation pleagues for an influence of proteins of the complete medium on the precipitation process. This result is consistent with SEM images that showed a different morphology of the precipitated layer on the TCP-T surface in presence of CM.

The presence of OCP phases on TCP-T substrates after immersion is not unfavorable for future tissue integration. Indeed, several studies have concerned the development of OCP-based biomaterials in various forms because of its high degradability compared with HA.[25-27] Moreover, in bioceramic field, it is known that the "unwanted" calcium orthophosphates (DCP, DCPD, etc.) are often present and coexist with other calcium orthophosphate phases (HA, TCP and OCP) and that some of them can be precursor of HA.[28,29]

The XPS data showed also that in the presence of CM, the percentage of Ca^{2+} and PO_4^{3-} was low because of the protein overlayer due to adsorption. No Mg^{2+} ions were detected in the newly formed layer over the 9 nm analysis depth of the XPS technique. On the contrary, in the presence of NCM medium, the N1s signal was logically very low, given the small amount of amino acids present in the NCM. Moreover, the precipitated overlay formed in static and dynamic conditions did content a low percentage of Mg^{2+} and Na^{+} ions (**Table 2**). The small magnesium content was explained by the precipitation of $MgSO_4$ salts present in culture medium. While sodium was present in large quantity in the culture medium, we can note that it was precipitated in a relatively low quantity. These results confirm our SEM-EDX data and other previous results we obtained on HA and HA doped with Si after immersion in similar biomimetic conditions.[15,16]

Biomimetic cell study. We know that the bone tissue is continuously perfused by interstitial liquid at 2 ml/h and continuously remodeled by the coordinated action of osteoblasts and osteoclasts.

Dynamic culture bioreactors such flow perfusion systems give a homogeneous distribution of medium that most times stimulate the proliferation and differentiation of cells.[30] Furthermore, these systems ensure a continuous nutrition and removal of waste products as well as mechanical stimuli of cells.

We can note that after 7 d, the number of cells was higher on TCP than on TCP-T samples whatever the culture conditions (**Fig. 7A**). This result is in contradiction with the observations we have done previously where the proliferation was increased by dynamic culture conditions of SaOs-2 cells on HA and HA-Si samples.[16] On the other hand, the differentiation of cells, after 7 d (their alkaline phosphatase activity) was higher on TCP-T than on TCP whatever the culture conditions (**Fig. 7B**).

Comparable studies done in static conditions showed that maturation and cellular differentiation could be accompanied by a decrease of cell proliferation for a given surface.[31,32] Thus it appears that the differentiation process of SaOs-2 cells was sped up on TCP-T compared with TCP while their proliferation was slowed down. Similarly a significant reduction of bone marrow stromal cells (BMSC) doublings was found by Scaglione et al.[33] when they were exposed to two different substrates (uncoated glass or calcium phosphate coated glass) in a fluid flow bioreactor. BMSC cultured under flow were more intensely stained for collagen type I and by Von Kossa for mineralized matrix. The alkaline phosphatase activity was decreased in the dynamic mode for both surfaces while the mRNA expressions of osteopontin, osteocalcin and bone sialoprotein were only dependent on the substrate used. This illustrates that differentiation markers can be differently modified by culture conditions. Moreover, attention must be paid to the cellular model as to the bioreactor system used.

Materials and Methods

Production of tablets. TCP stoichiometric powder was prepared by aqueous precipitation technique using a diammonium phosphate solution $(NH_4)_2HPO_4$ (Carlo Erba) and a calcium nitrate solution $Ca(NO_3)_2\ 4H_2O$ (Brenntag) with an initial Ca/P ratio equal to 1.5 for obtaining stoichiometric β-TCP powder.[34] For TCP synthesis, the pH of the solution was adjusted at a constant value to 6.5 by a continuous addition of ammonium hydroxide and the temperature was fixed to 30°C. After maturation during 24 h, solutions were filtered and the precipitates were dried to 70°C.

The phase composition of the powder was characterized using X-ray powder diffraction (Rigaku Miniflex). The XRD spectrum, performed under 30 kV and 15 mA exciting and using a Cu anticathode, was collected between 20–60°C (2θ) with a step width of 0.02°C, a count time to 20 sec. Infrared spectra of the powder recorded on a Fourier transform spectrometer (Jasco-FT/IR-460 Plus) were used for detection of the presence of pyrophosphate group ($Ca_2P_2O_7$ or CPP) in TCP phase.

Powder obtained with this synthesis underwent a calcination treatment at 750°C which was followed by a grinding with a ball milling during 3 h to break up agglomerates formed during calcination. After this treatment, the specific surface area of ground powders was recorded by the BET method (Micromeritics, Flow Sorb 3), which uses the physical adsorption of gas molecules on solid surface to determine the characteristic.

TCP compacts were obtained by slip casting process. Aqueous slurry was prepared with a powder concentration equal to 65 wt.% and dispersion of the powder was assured by a commercial organic agent (Darvan C, R.T. Vanderbilt Co.) in amount equal to 1.5 wt.% of powder content.

In a first step, TCP tablets (Φ = 13 mm, e = 2.5 mm) were pressureless sintered at 1,060°C for 3 h in air atmosphere. Heating and cooling rates were fixed to 300°C/h. In a second step, to complete the sample densification and to reach a density close to theoretical density, pre-sintered samples were hipped (HIP). Trials were performed in GPS VITEK HIP equipped with a platinum furnace, under Ar/O_2 atmosphere (80/20 vol.%). The HIP treatment conditions were a temperature of 1,050°C, a

heating rate of 300°C/min and an isostatic pressure of 150 MPa for 1 h.

The relative density of pressureless sintered (TCP) and hipped samples (TCP-T) was determined by hydrostatic weighing using the Archimedes' method. Microstructure pictures of these samples were performed by scanning electron microscopy (Hitachi S-3500N) after a mirror polishing and a thermal etching performed in air at a temperature 50°C below the sintering temperature.

Biomimetic immersion study. *Immersion in static condition.* In order to study the surface transformation of materials after immersion in static condition, the samples were put in classical 24-well plates for cell culture and incubated into a CO_2 cell culture incubator (Hera Cell) at 37°C. The samples were immersed in 1 mL McCoy's non-complete medium (NCM) (Sigma) or complete medium (CM) (added with 10% fetal bovine serum) (VWR) for 1, 3 and 8 d.

Immersion in dynamic condition. For dynamic conditions, it was used a Minucells® flow perfusion bioreactor (MINUCELLS and MINUTISSUE) inside a CO_2 cell culture incubator (HeraCell) at 37°C. The system consists of a chamber, supplied by medium by a peristaltic pump (Type IPC-N8 from ISMATEC) at a 2 mL/h flow rate. Complete or non-complete medium (McCoy's, Sigma) flows between the ceramic samples vertically in a bottom-up direction. The pH of solutions was verified to be constant, 7.4, each day.

The whole system was sterilized before each experiment at 105°C and 1 bar pressure in an autoclave apparatus for eliminating any kind of contamination. The whole system was assembled under sterile hood and the first bottle was filled with fresh, sterile complete or non-complete McCoy's medium.

After static or dynamic immersion, the samples were removed from the solutions, washed with distilled water and then dried in air, under sterile hood. For every characterization, the pristine TCP and TCP-T plates were used as controls.

Surface characterization after biomimetic immersion study. The morphology of TCP and TCP-T after biomimetic immersion study was examined by scanning electron microscopy (SEM) in a JEOL JSM 6460LV microscope to investigate the surface transformations. The analysis was done once and the most representative pictures of each samples were selected. The analysis of the surface chemistry was performed in the same time using an EDX system coupled to the scanning electron microscope.

XPS. X-ray photoelectron spectroscopy (XPS) was also used to follow modifications of the surface chemistry after fluid immersion. Analysis was performed using a Gammadata Scienta SES 2002 X-ray photoelectron spectrometer under ultra high vacuum ($p < 10^{-9}$ mbar). The monochromated Al Kα source (1486.6 eV) was operated at 420 W (30 mA, 14 kV), with a nominal take-off angle of 90° (i.e., photoelectrons ejection normal to the surface). The samples were outgassed into several ultra high vacuum chambers with isolated pumping system until transfer to the analysis chamber. No further cleaning process was made to avoid carbon contamination. During acquisition, the pass energy was set to 500 eV for survey spectrum with a step of 500 meV. The overall energetic resolution of the spectrometer can be estimated to 0.4 eV. For quantification purpose, raw area of each photoelectron peaks was determined on survey spectrum using Shirley background and 30% Gaussian-Lorentzian shape with CasaXPS software (Casa Software Ltd.). Raw areas were further modified using classical sensitivity factors and transmission factor of the spectrometer leading to a chemical composition expressed in atomic percentage in the article. The analysis depth of XPS is approximately 8–9 nm.

XPS surface characterization was performed only for the T-TCP samples (one sample for each condition): the control T-TCP (pristine sample) and samples immersed in static or dynamic conditions, in complete and non-complete medium during 8 d (total five samples).

Calcium and phosphorous content in medium. The concentration of calcium and phosphorus in the immersion medium after contact with the TCP and T-TCP tablets was evaluated at the end of each immersion time (1, 3 and 8 d) by colorimetric methods using a Calcium AS FS kit and Phosphorus UV FS kit purchased by Diasys Diagnostic Systems.

Protein concentration in medium. The concentration of total proteins in the immersion medium after contact with the TCP and T-TCP tablets was evaluated at the end of each immersion time (1, 3 and 8 d) by the Micro BCA™ kit using the supplier instructions (Pierce). Protein concentration was obtained by comparison with BSA standards.

Biomimetic cell culture study. The present study used the human osteosarcoma-derived osteoblastic cell line SaOs-2. The cells were cultured in McCoy's medium (Eurobio) supplemented with 10% fetal bovine serum (Eurobio) and 100 U/mL of Penicillin and 100 µg/mL of Streptomycin (Eurobio). The cells were kept in an incubator at 37°C under a humidified atmosphere of 95% air and 5% CO_2. At confluence, the cells were detached by trypsinization with 0.25% crude trypsin and 0.02% EDTA, pH 7.2.

Static and dynamic cell culture. After trypsinization, 4.0×10^4 SaOs-2 cells were seeded on each sample into a 24-well plate coated with agar gel (2% in water) to avoid cell growth on the bottom of the well. After 24 h of incubation in order to let the cells adhere on the samples, half of the samples were transferred inside the Minucells® flow perfusion bioreactor (MINUCELLS and MINUTISSUE), for dynamic cell culture as previously described.[15,16] The comparative study was done in parallel with the other half of samples let into the static 24-well culture plates. At the end of each period, the cells on samples were either treated for immunofluorescence, for proliferation assay and for differentiation assay. A total of three independent assays were performed for each experiment, with each assay performed in triplicate.

Actin cytoskeleton formation. After 3 d of culture, the cells were fixed with 2% paraformaldehyde for 30 min. They were washed with PBS, permeabilized with 0.2% Triton X-100 in PBS for 15 min, and washed again with PBS. The samples were then incubated in 1% albumin solution (in PBS) for 20 min at room temperature to block non-specific adsorption, washed three times with PBS (5 min each). After these steps, the cells were incubated with FITC-phalloidin (0.4 µg/ml, Sigma, France) for 1 h at room

temperature and washed again with PBS. Then, the cells were incubated with a DAPI solution (100 ng/mL) for 20 min at room temperature to label their nucleus. Samples were examined with a microscope Olympus BX 51 equipped with epifluorescence (Olympus).

MTT assay. The cells were monitored after 1, 3 and 7 d in culture. At each time point, the samples were slightly rinsed with PBS solution to remove non adhered cells. One thousand microliters of 5 mg/mL MTT [3-(4,5-dimethylthiazol-2-yl)-2,5-diphenyl tetrazolium bromide] (Sigma) were added to the adherent cells and incubated for 3 h at 37°C under a humidified atmosphere of 95% air and 5% CO_2. Afterwards, the MTT was removed and the cells were immersed in 300 µL of acidic isopropanol under shaking to dissolve intracellular formazan crystals produced by viable cells. Absorbance was determined at 570 nm using an ELISA plate reader. Cell number was obtained using a linear correlation between absorbance and SaOs2 cell concentration (from 0.5×10^4 up to 2×10^4 cells/mL). The cell number was adjusted to the surface of samples and was expressed in cells/mm^2. The results from three individual experiments (in triplicate) were averaged.

Alkaline phosphatase assay. Alkaline phosphatase (ALP) activity was assessed by the hydrolysis of *p*-nitrophenyl phosphate in alkaline buffer solution (substrate). After 1, 3 and 7 d in culture, the cells plated on the surfaces were previously permeabilized in 0.5% Triton X-100 (octylphenol ethoxylate) in water and incubated for 30 min with the substrate. Colorimetric determination of the product (*p*-nitrophenol) was performed at 405 nm (ELISA reader). ALP activity was calculated from a standard curve, and the results were expressed in nanomoles of *p*-nitrophenol produced per cell (nmol L^{-1}/cell).

Statistical significance. The statistical significance of the obtained data was assessed using two-way ANOVA variance analysis. Level of significance was set at $p < 0.05$.

Conclusions

Thanks to the biomimetic immersion study we proposed, we were able to appreciate the surface transformation of sintered TCP and hipped TCP-T tablets after static and dynamic immersion in biological fluids containing or not proteins. The quantity of apatite precipitates was higher in dynamic conditions that in static conditions. The deposition of apatite layer was larger and faster on TCP-T compared with TCP, but was impeded by proteins present in CM medium. Regarding the biomimetic cell study on these two materials, the cellular morphology was not affected by the nature of the samples or the culture conditions. Finally, the densification of tricalcium phosphate bioceramic by hot isostatic pressing treatment (HIP) did not alter significantly the biological properties of the material.

Again, it was demonstrated that the biomimetic approach is an effective tool for predicting surface transformation after in vitro immersion in simulated body fluids in conditions closer to in vivo conditions (dynamic immersion in presence of proteins) and the cellular behavior on bioactive materials with medical application.

Disclosure of Potential Conflicts of Interest

No potential conflicts of interest were disclosed.

References

1. Lange T, Schilling AF, Peters F, Mujas J, Wicklein D, Amling M. Size dependent induction of proinflammatory cytokines and cytotoxicity of particulate beta-tricalciumphosphate in vitro. Biomaterials 2011; 32: 4067-75; PMID:21421269; http://dx.doi.org/10.1016/j.biomaterials.2011.02.039
2. Knabe C, Koch C, Rack A, Stiller M. Effect of beta-tricalcium phosphate particles with varying porosity on osteogenesis after sinus floor augmentation in humans. Biomaterials 2008; 29:2249-58; PMID:18289665; http://dx.doi.org/10.1016/j.biomaterials.2008.01.026
3. Weinand C, Pomerantseva I, Neville CM, Gupta R, Weinberg E, Madisch I, et al. Hydrogel-beta-TCP scaffolds and stem cells for tissue engineering bone. Bone 2006; 38:555-63; PMID:16376162; http://dx.doi.org/10.1016/j.bone.2005.10.016
4. Cao H, Kuboyama N. A biodegradable porous composite scaffold of PGA/beta-TCP for bone tissue engineering. Bone 2010; 46:386-95; PMID:19800045; http://dx.doi.org/10.1016/j.bone.2009.09.031
5. Yang Y, Zhao Y, Tang G, Li H, Yuan X, Fan Y. In vitro degradation of porous poly(l-lactide-co-glycolide)/β-tricalcium phosphate(PLGA/β-TCP) scaffolds under dynamic and static conditions. Polym Degrad Stabil 2008; 93:1838-45; http://dx.doi.org/10.1016/j.polymdegradstab.2008.07.007
6. Alcaide M, Serrano MC, Pagani R, Sánchez-Salcedo S, Vallet-Regí M, Portolés MT. Biocompatibility markers for the study of interactions between osteoblasts and composite biomaterials. Biomaterials 2009; 30: 45-51; PMID:18838165; http://dx.doi.org/10.1016/j.biomaterials.2008.09.012
7. Arnold U, Lindenhayn K, Perka C. In vitro-cultivation of human periosteum derived cells in bioresorbable polymer-TCP-composites. Biomaterials 2002; 23:2303-10; PMID:12013177; http://dx.doi.org/10.1016/S0142-9612(01)00364-7
8. Sánchez-Salcedo S, Balas F, Izquierdo-Barba I, Vallet-Regí MF. In vitro structural changes in porous HA/beta-TCP scaffolds in simulated body fluid. Acta Biomater 2009; 5:2738-51; PMID:19394904; http://dx.doi.org/10.1016/j.actbio.2009.03.025
9. Ryu HS, Hong KS, Lee JK, Kim DJ, Lee JH, Chang BS, et al. Magnesia-doped HA/beta-TCP ceramics and evaluation of their biocompatibility. Biomaterials 2004; 25:393-401; PMID:14585687; http://dx.doi.org/10.1016/S0142-9612(03)00538-6
10. Yamada S, Heymann D, Bouler JM, Daculsi G. Osteoclastic resorption of calcium phosphate ceramics with different hydroxyapatite/beta-tricalcium phosphate ratios. Biomaterials 1997; 18:1037-41; PMID: 9239465; http://dx.doi.org/10.1016/S0142-9612(97)00036-7
11. Xie Y, Hardouin P, Zhu Z, Tang T, Dai K, Lu J. Three-dimensional flow perfusion culture system for stem cell proliferation inside the critical-size β-tricalcium phosphate scaffold. Tissue Eng 2006; 12:3535-43; PMID:17518689; http://dx.doi.org/10.1089/ten.2006.12.3535
12. Zhao J, Watanabe T, Bhawal UK, Kubota E, Abiko Y. Transcriptome analysis of β-TCP implanted in dog mandible. Bone 2011; 48:864-77; PMID:21134491; http://dx.doi.org/10.1016/j.bone.2010.11.019
13. Zhang M, Wang K, Shi Z, Yang H, Dang X, Wang W. Osteogenesis of the construct combined BMSCs with beta-TCP in rat. J Plast Reconstr Aesthet Surg 2010; 63:227-32; PMID:19091642; http://dx.doi.org/10.1016/j.bjps.2008.11.017
14. Chappard D, Guillaume B, Mallet R, Pascaretti-Grizon F, Baslé MF, Libouban H. Sinus lift augmentation and beta-TCP: a microCT and histologic analysis on human bone biopsies. Micron 2010; 41:321-6; PMID: 20060730; http://dx.doi.org/10.1016/j.micron.2009.12.005
15. da Silva HM, Mateescu M, Ponche A, Damia C, Champion E, Soares G, et al. Surface transformation of silicon-doped hydroxyapatite immersed in culture medium under dynamic and static conditions. Colloids Surf B Biointerfaces 2010; 75:349-55; PMID: 19800204; http://dx.doi.org/10.1016/j.colsurfb.2009.09.009
16. da Silva HM, Mateescu M, Damia C, Champion E, Soares G, Anselme K. Importance of dynamic culture for evaluating osteoblast activity on dense silicon-substituted hydroxyapatite. Colloids Surf B Biointerfaces 2010; 80:138-44; PMID:20579858; http://dx.doi.org/10.1016/j.colsurfb.2010.05.040
17. Tanimoto Y, Hayakawa T, Sakae T, Nemoto K. Characterization and bioactivity of tape-cast and sintered TCP sheets. J Biomed Mater Res A 2006; 76:571-9; PMID:16278874; http://dx.doi.org/10.1002/jbm.a.30558

18. Lu HB, Campbell CT, Graham DJ, Ratner BD. Surface characterization of hydroxyapatite and related calcium phosphates by XPS and TOF-SIMS. Anal Chem 2000; 72:2886-94; PMID:10905323; http://dx.doi.org/10.1021/ac990812h
19. Juhasz JA, Best SM, Auffret AD, Bonfield W. Biological control of apatite growth in simulated body fluid and human blood serum. J Mater Sci Mater Med 2008; 19:1823-9; PMID:18157508; http://dx.doi.org/10.1007/s10856-007-3344-7
20. Bohner M, Lemaitre J. Can bioactivity be tested in vitro with SBF solution? Biomaterials 2009; 30:2175-9; PMID:19176246; http://dx.doi.org/10.1016/j.biomaterials.2009.01.008
21. Porter AE, Patel N, Skepper JN, Best SM, Bonfield W. Comparison of in vivo dissolution processes in hydroxyapatite and silicon-substituted hydroxyapatite bioceramics. Biomaterials 2003; 24:4609-20; PMID:12951004; http://dx.doi.org/10.1016/S0142-9612(03)00355-7
22. Rámila A, Vallet-Regí M. Static and dynamic in vitro study of a sol-gel glass bioactivity. Biomaterials 2001; 22:2301-6; PMID:11456070; http://dx.doi.org/10.1016/S0142-9612(00)00419-1
23. Radin S, Ducheyne P, Rothman B, Conti A. The effect of in vitro modeling conditions on the surface reactions of bioactive glass. J Biomed Mater Res 1997; 37:363-75; PMID:9368141; http://dx.doi.org/10.1002/(SICI)1097-4636(19971205)37:3<363::AID-JBM7>3.0.CO;2-J
24. Radin S, Ducheyne P. Effect of serum proteins on solution-induced surface transformations of bioactive ceramics. J Biomed Mater Res 1996; 30:273-9; PMID:8698689; http://dx.doi.org/10.1002/(SICI)1097-4636(199603)30:3<273::AID-JBM1>3.0.CO;2-N
25. Shelton RM, Liu Y, Cooper PR, Gbureck U, German MJ, Barralet JE. Bone marrow cell gene expression and tissue construct assembly using octacalcium phosphate microscaffolds. Biomaterials 2006; 27:2874-81; PMID:16439012; http://dx.doi.org/10.1016/j.biomaterials.2005.12.031
26. Kikawa T, Kashimoto O, Imaizumi H, Kokubun S, Suzuki O. Intramembranous bone tissue response to biodegradable octacalcium phosphate implant. Acta Biomater 2009; 5:1756-66; PMID:19136321; http://dx.doi.org/10.1016/j.actbio.2008.12.008
27. Miyatake N, Kishimoto KN, Anada T, Imaizumi H, Itoi E, Suzuki O. Effect of partial hydrolysis of octacalcium phosphate on its osteoconductive characteristics. Biomaterials 2009; 30:1005-14; PMID:19027945; http://dx.doi.org/10.1016/j.biomaterials.2008.10.058
28. Eliaz N, Kopelovitch W, Burstein L, Kobayashi E, Hanawa T. Electrochemical processes of nucleation and growth of calcium phosphate on titanium supported by real-time quartz crystal microbalance measurements and X-ray photoelectron spectroscopy analysis. J Biomed Mater Res A 2009; 89:270-80; PMID:18563813; http://dx.doi.org/10.1002/jbm.a.32129
29. Dorozhkin SV. Bioceramics of calcium orthophosphates. Biomaterials 2010; 31:1465-85; PMID:19969343; http://dx.doi.org/10.1016/j.biomaterials.2009.11.050
30. Yeatts AB, Fisher JP. Bone tissue engineering bioreactors: dynamic culture and the influence of shear stress. Bone 2011; 48:171-81; PMID:20932947; http://dx.doi.org/10.1016/j.bone.2010.09.138
31. Tamada Y, Ikada Y. Fibroblast growth on polymer surfaces and biosynthesis of collagen. J Biomed Mater Res 1994; 28:783-9; PMID:8083246; http://dx.doi.org/10.1002/jbm.820280705
32. Suh H, Hwang YS, Lee JE, Han CD, Park JC. Behavior of osteoblasts on a type I atelocollagen grafted ozone oxidized poly L-lactic acid membrane. Biomaterials 2001; 22:219-30; PMID:11197497; http://dx.doi.org/10.1016/S0142-9612(00)00177-0
33. Scaglione S, Wendt D, Miggino S, Papadimitropoulos A, Fato M, Quarto R, et al. Effects of fluid flow and calcium phosphate coating on human bone marrow stromal cells cultured in a defined 2D model system. J Biomed Mater Res A 2008; 86:411-9; PMID:17969030; http://dx.doi.org/10.1002/jbm.a.31607
34. Descamps M, Hornez JC, Leriche A. Manufacture of hydroxyapatite beads for medical applications. J Eur Ceram Soc 2009; 29:2401-6; http://dx.doi.org/10.1016/j.jeurceramsoc.2008.06.008